

Lockdowns exert selection pressure on overdispersion of SARS-CoV-2 variants

Bjarke Frost Nielsen^a, Andreas Eilersen^a, Lone Simonsen^b, and Kim Sneppen^{a,2}

^aNiels Bohr Institute, University of Copenhagen, Blegdamsvej 17, 2100 Copenhagen, Denmark.; ^bDepartment of Science and Environment, Roskilde University, Universitetsvej 1, 4000 Roskilde, Denmark.

Preprint dated June 30, 2021

The SARS-CoV-2 ancestral strain has caused pronounced superspreading events, reflecting a disease characterized by overdispersion, where about 10% of infected people causes 80% of infections. New variants of the disease have different person-to-person variations in viral load, suggesting for example that the Alpha (B.1.1.7) variant is more infectious but relatively less prone to superspreading. Meanwhile, mitigation of the pandemic has focused on limiting social contacts (lockdowns, regulations on gatherings) and decreasing transmission risk through mask wearing and social distancing. Using a mathematical model, we show that the competitive advantage of disease variants may heavily depend on the restrictions imposed. In particular, we find that lockdowns exert an evolutionary pressure which favours variants with lower levels of overdispersion. We find that overdispersion is an evolutionarily unstable trait, with a tendency for more homogeneously spreading variants to eventually dominate.

Overdispersion | Evolution | Superspreading | Non-pharmaceutical interventions

One of the major features of the coronavirus pandemic has been overdispersion in transmission, manifesting itself as superspreading. There is evidence that around 10% of infected individuals are responsible for 80% of new cases (1–4). This means that some individuals have a high personal reproductive number, while the majority hardly infect at all. A recent study has shown this is reflected in the distribution of viral loads which is extremely wide, with just 2% of SARS-CoV-2 positive individuals carrying 90% of the virus particles circulating in communities (5). Overdispersion is in fact a key characteristic of certain diseases (6–8). However, this is by no means a universal signature of infectious respiratory diseases. Pandemic influenza, for example, is characterized by a much more homogeneous transmission pattern (9–11).

As an emerging virus evolves, its transmission patterns may change and it may become more or less prone to superspreading. The Alpha (B.1.1.7) variant of SARS-CoV-2 has been reported to be ~ 50% more transmissible than the ancestral SARS-CoV-2 virus under varying degrees of lockdown (12–14). Meanwhile, others have shown that the Alpha variant possesses a higher average viral load and a reduced variability between infected persons, compared to the ancestral strain (15, 16). It remains to be seen how this reduced variability affects the transmission patterns of the virus.

The altered viral load distributions seen in persons infected with the Alpha variant have also been investigated at the level of individual mutations. The spike protein of the Alpha variant prominently features the N501Y substitution (asparagine replaced by tyrosine at the 501 position) as well as the Δ H69/V70 deletion (histidine and valine deleted at the 69 and 70 positions). Investigators found that the viral

load is, on average, three times as great for the Alpha variant compared with the ancestral strain (16). Furthermore, viral load distributions in samples taken from persons infected with a variant with the Δ H69/V70 show a lower variance, whether or not they also have tyrosine at the 501 position. However, the difference in variance was most pronounced for those samples which had the deletion as well as the 501Y mutation. Similarly, an analysis of samples with the N501Y mutation show that they have a higher median viral load as well as a substantially diminished variance compared to those without it. Using data from Ref. (15), we calculate that the viral loads in samples of the Alpha variant are associated with a lower coefficient of variation of approximately 2, compared to 4 for the ancestral strain. Importantly, the exact relation between viral load and infectiousness is not well understood; however, a higher viral load is logically expected to increase the risk of disease transmission. By this logic, the decreased variability in the viral load for the Alpha variant may translate into a reduced overdispersion in transmission.

In this paper, we use a mathematical model to study the competition between idealized variants which differ in their level of overdispersion (k) and their mean infectiousness. Our focus is on exploring whether overdispersion confers any evolutionary (dis)advantages, and whether non-pharmaceutical interventions which restrict social network size and transmissibility change the fitness landscape for variants with varying degrees of overdispersion. While it is evident that a higher mean infectiousness confers an evolutionary advantage to an emerging pathogen, it is not *a priori* obvious if a competitive

Significance

One of the most important and complex properties of viral pathogens is their ability to mutate. The SARS-CoV-2 pandemic has been characterized by overdispersion – a propensity for superspreading, which means that around 10% of those who become infected cause 80% of infections. However, evidence is mounting that this is not a stable property of the virus and that the Alpha variant spreads more homogeneously. We use a mathematical model to show that lockdowns exert a selection pressure, driving the pathogen towards more homogeneous transmission. In general, we highlight the importance of understanding how non-pharmaceutical interventions exert evolutionary pressure on pathogens. Our results imply that overdispersion should be taken into account when assessing the transmissibility of emerging variants.

The authors declare no competing interests.

²To whom correspondence should be addressed. E-mail: sneppen@nbi.dk

61 advantage can be gained by specifically altering the *variability*
 62 in infectiousness (while keeping transmissibility unchanged).
 63 Our recent studies have shown that the presence of overdispersion
 64 makes a pandemic far more controllable than influenza
 65 pandemics when mitigating by limiting non-repetitive contacts
 66 (17) and personal contact network size (18). We therefore speculate
 67 that restrictions which alter social contact structure may,
 68 conversely, provide a fitness advantage to variants with more
 69 homogeneous transmission, and may thus play a role in viral
 70 evolution.

71 Across several diseases, individual variations in infectiousness
 72 have been approximated by a Gamma distribution (6)
 73 characterized by a certain mean value and a dispersion
 74 parameter known as k , which is related to the coefficient of
 75 variation (CV) through $CV = 1/\sqrt{k}$. In the simplest of cases
 76 (a well-mixed population), infection attempts are modeled as
 77 a constant-rate (Poisson) process, which leads to a personal
 78 reproductive number which follows a negative binomial distribution.
 79 The dispersion parameter k characterizes the degree of
 80 transmission heterogeneity; a *lower* k corresponds to greater
 81 heterogeneity. For small values of k , it approximately corresponds
 82 to the fraction of infected individuals responsible for
 83 80% of new infections. The value for the SARS-CoV-2 ancestral
 84 virus is around 10%, corresponding to a k -value of approximately
 85 0.1. Other coronaviruses are also prone to superspreading,
 86 with the k -values of SARS-CoV-1 and MERS estimated
 87 at 0.16 (6) and 0.26 (19), respectively. To explore questions of
 88 how such overdispersion affects fitness and pathogen evolution,
 89 we use an agent-based model of COVID-19 spreading in a
 90 social network, as originally developed in Ref. (18).

91 Overdispersion in personal reproductive number – i.e. superspreading –
 92 is a phenomenon that requires *means* (biological infectiousness)
 93 as well as *opportunity* (social context). Superspreading can have
 94 diverse origins, ranging from purely behavioural to biological (8, 20).
 95 However, a recent meta-review (21) compared the transmission
 96 heterogeneity of influenza A (H1N1), SARS-CoV-1 and SARS-CoV-2
 97 and found that higher variability in respiratory viral load was
 98 closely associated with increased transmission heterogeneity. This
 99 suggests that biological aspects of individual diseases are decisive
 100 in determining the level of overdispersion, and thus the risk of
 101 superspreading.
 102

103 Initial survival of variants

104 The words *fitness* and *competitive advantage* may take on
 105 several meanings in an evolutionary context. For our purposes,
 106 it is especially important to distinguish between the ability
 107 of a pathogen to *avoid stochastic extinction* and to *reproduce*
 108 *effectively* in a population.

109 To quantify the ability to avoid stochastic extinction we
 110 use a branching process to simulate an outbreak of a variant
 111 with a given level of overdispersion in a naive population. We
 112 then record whether it survives beyond the first 10 generations
 113 of infections, as a measure of the ability of that variant to take
 114 hold. Repeating these simulations multiple times allows us
 115 to compute the survival chance of each variant as a function
 116 of its infectiousness and overdispersion, in the absence and
 117 presence of mitigation (Fig. 1). Since we are dealing with a
 118 few related quantities, some definitions must be made. By
 119 the *basic reproductive number* (R_0) we mean the average number
 120 of new infections which each infected person gives rise to

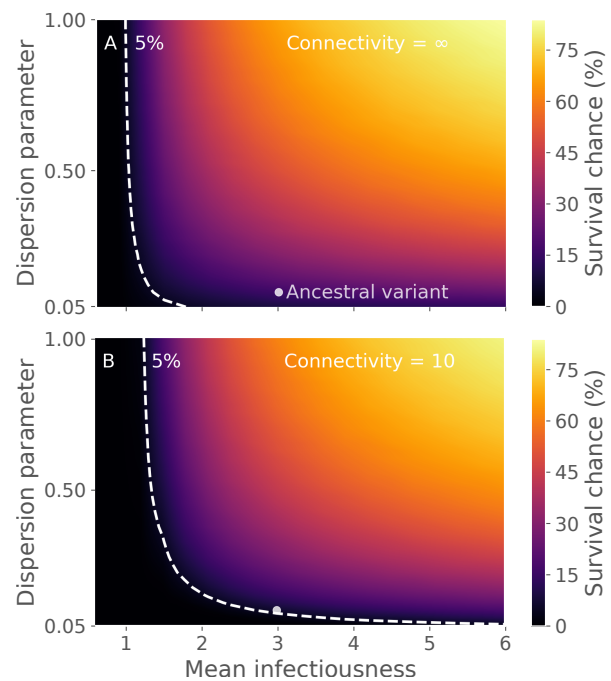


Fig. 1. Initial survival chance depends strongly on overdispersion and moderately on lockdown status. **A)** The epidemic spreads in an unrestricted setting (homogeneous mixing contact structure) **B)** The epidemic spreads in a situation with limited social connectivity (modeled as an Erdos-Renyi network of average connectivity 10). The survival chance is computed by simulating several outbreaks, each starting from a single infected individual in a susceptible population. This initial individual is infected with a variant of a given overdispersion. For each outbreak, the variant is recorded as having *survived* if it does not go extinct within 10 generations. The dashed white line indicated parameters for which the variant has a 5% chance of surviving. The biological mean infectiousness (horizontal axis) has been scaled such that it equals the basic reproductive number (R_0) in the homogeneous mixing scenario of panel A. For details on these calculations, see the Materials and Methods section.

121 *when all contacts are susceptible*. This is in contrast to the
 122 effective reproductive number (known variously as R , R_t and
 123 R_e), which is affected by population immunity. Note that R_0
 124 as well as R_e are context dependent, since behaviour (and
 125 mitigation strategies) will affect e.g. the number of contacts
 126 that a person has and thus the reproductive number. Another
 127 parameter entirely is the (*biological*) *mean infectiousness*, by
 128 which we mean the rate at which transmission occurs *when*
 129 an infected person is in contact with a susceptible person. This
 130 is a property of the disease and not of the social environment. In
 131 Fig. 1, the independent variables are thus the mean infectiousness
 132 and the dispersion parameter, both of which are assumed to be
 133 properties of the disease. The details of the calculation
 134 can be found in the Materials and Methods section.

135 In the unmitigated scenario (Fig. 1A), the procedure is relatively
 136 straightforward. A single infected individual is initially
 137 introduced, with a personal reproductive number z drawn from
 138 a negative binomial distribution $P_{NB}[Z; R_0, k]$ with mean value
 139 R_0 and dispersion parameter k . Thus, this individual gives
 140 rise to z new cases, and the algorithm is reiterated for each of
 141 these subsequent infections.

142 In the case of a lockdown scenario, in terms of restrictions
 143 of the number of social contacts (Fig. 1B), the algorithm is
 144 slightly more involved. In this case, a *degree* c (the number of
 145 contacts) is first drawn from a degree distribution (in this case

146 a Poisson distribution, to mimic an Erdős-Renyi network). A
 147 biological reproductive number ξ (the *infectiousness*) is then
 148 drawn from a Gamma distribution with mean value R_0 and
 149 dispersion parameter k . The actual personal reproductive
 150 number z is then drawn from the distribution

$$151 \quad P(z; \xi, c) = \binom{c}{z} (1 - e^{-\xi/c})^z (e^{-\xi/c})^{(c-z)}. \quad [1]$$

152 This reflects that the personal reproductive number z is, natu-
 153 rally enough, limited by the number of distinct social contacts
 154 c . This algorithm is then reiterated for each of the z new
 155 cases.

156 Similar results can be obtained analytically by considering
 157 the probability that an infection chain dies out in infinite
 158 time. Let that probability be d and let $p_i, i \in \{0, 1, \dots\}$ be
 159 the distribution of personal reproductive number (i.e. p_i is
 160 the probability that a single infected individual will infect i
 161 others). Then the extinction risk d is the sum:

$$162 \quad d = p_0 + p_1 d + p_2 d^2 + \dots \quad [2]$$

163 where the first term on the right hand side is the extinction
 164 risk due to the index case producing no new infections, the
 165 second term is the case where the index case gives rise to
 166 one branch of infections which then dies out (this being the
 167 reason for the single factor of d in the second term) and so on.
 168 Since each new branch exists independently of the other, the
 169 extinction events are independent and the probabilities may
 170 be combined by simple multiplication as in Eq. (2).

171 We find that the survival chance depends very strongly
 172 on overdispersion (Fig. 1), with more homogeneous variants
 173 ($k \sim 1$) having a good chance of survival while highly overdis-
 174 persed variants ($k \leq 0.1$) are very unlikely to survive beyond
 175 10 generations. This finding fits well with the general pat-
 176 tern of overdispersed spreading, namely that many individuals
 177 hardly become infectious while a few pass the disease onto
 178 many others. The uneven distribution of infectiousness makes
 179 heterogeneous diseases more fragile in the early stages of an
 180 epidemic, and thus more prone to stochastic extinction.

181 For the case of homogeneous mixing (Fig 1A) and the num-
 182 ber of generations tending to infinity, Lloyd-Smith et al (6)
 183 performed a similar calculation using the generating function
 184 method described in Eq. 2. For a disease with $R_0 = 3$ and a k
 185 value of 0.16 (similar to what they estimated for SARS-CoV-1),
 186 the survival chance was found to be 24%. Our model yields
 187 the same figure in the unmitigated connectivity $\rightarrow \infty$ limit.

188 To assess the effect of lockdown-like non-pharmaceutical
 189 interventions on the initial survival chances of a pathogen, we
 190 performed an analogous computation in a socially restricted
 191 setting (Fig. 1B). Compared with the unmitigated scenario of
 192 Fig. 1A, it can be seen that the mitigation has an effect on the
 193 survival chance, affecting highly overdispersed variants (small
 194 k) much more than their more homogeneous counterparts
 195 (with the same mean infectiousness). This result is parallel
 196 to the effect of lockdown-like interventions on the *competitive*
 197 *advantage* of a variant, which we explore in the next section.

198 In Ref. (20), the authors study stochastic extinction of
 199 a superspreading disease under a targeted intervention they
 200 call *cutting the tail*. They introduce a cutoff value N_{cutoff}
 201 for the personal reproductive number, and if a person has a
 202 personal reproductive number $z \geq N_{\text{cutoff}}$, a new z is drawn
 203 until one below the threshold is obtained. Since the disease is

highly heterogeneous, this process is analogous to "removing" 204
 a potential superspreading event and replacing it with a much 205
 lower personal reproductive number (typically $z = 0$). This is 206
 exactly why the intervention is rightly called *targeted*. Their 207
 approach is thus based on viewing superspreading entirely as 208
 an event-based phenomenon, where one can directly remove 209
 superspreading events above some threshold size, and instead 210
 let the individuals take part in other less risky events. Our 211
 approach, on the other hand, assumes superspreading to be 212
 due to a combination of high individual biological infectious- 213
 ness and opportunity, e.g. a large number of social contacts. 214
 These two viewpoints are complementary in obtaining a com- 215
 prehensive description of superspreading phenomena, rather 216
 than mutually exclusive (17). 217

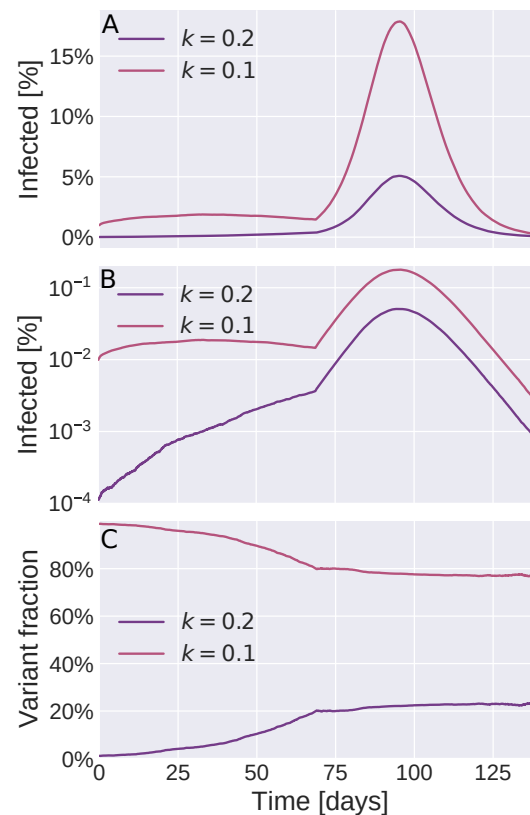


Fig. 2. Simulations of the emergence of a new variant. An initially dominant ("ancestral") strain with dispersion parameter $k = 0.1$ (red) has initially infected 1% of the population. The figure follows the emergence of a new variant (purple), which has the same biological mean infectiousness, but is more homogeneous ($k = 0.2$). Initially, 0.01% of the population is infected with the emerging variant. The two variants exhibit perfect cross-immunity. The initial scenario is a partially locked-down society (modeled as an Erdős-Renyi network with 10 contacts/person). When the new variant reaches 20% of all current infections (around day 65), the lockdown is completely lifted (modeled by a homogeneous mixing contact structure with the same *total* social time available per person). **A**) Incidence of each strain as a function of time since the new variant was introduced. Notice that the new variant spreads approximately exponentially until day 65 (see also panel B), whereas the ancestral strain stays at about 1% incidence. When restrictions are lifted, both surge. **B**) Same data as panel A, but plotted on a logarithmic scale. In this plot, exponential growth shows up as a straight line, and it is thus clear that the new variant spreads approximately exponentially during the lockdown phase. **C**) The relative proportions of the old and new variants. In the locked-down society, the new variant has a distinct fitness advantage, as revealed by its increasing share of infections. Once restrictions are lifted around $t = 65$ days, the fitness advantage is lost and the two variants spread equally well.

218 Competitive advantage is determined by context

219 We now turn to the competition between two variants which
220 have already managed to gain a foothold, and so have moved
221 past the initial risk of stochastic extinction. This is a separate
222 aspect of “fitness”, distinct from the initial survival ability
223 described in the last section. Fig. 2 explores the competi-
224 tion between two strains which differ only in their level of
225 overdispersion. The ancestral variant has a broad infectious-
226 ness distribution ($k = 0.1$) while the other – the *new variant* –
227 is more narrowly distributed ($k = 0.2$). In the initial partial
228 lockdown scenario, each person is only allowed contact with
229 10 others. At first, the fraction of infections due to the new
230 variant is observed to grow rapidly. When it reaches a 20%
231 share of active infections, around day 65, the lockdown is
232 lifted (simulated by a shift to a homogeneous mixing contact
233 structure). Naturally, this more permissive contact structure
234 causes a surge in both variants (Fig. 2c). However, the frac-
235 tion of infections owing to *each* variant suddenly stabilizes,
236 indicating that the more homogeneous new variant has lost
237 its competitive advantage in the unmitigated scenario.

238 This sudden loss of competitive advantage demonstrates
239 conceptually that the fitness of variants with different pat-
240 terns of overdispersion depends on context, in the form of
241 non-pharmaceutical interventions or the absence thereof. To
242 quantify this dependence, we separately simulate the spread
243 of several pathogen variants, each with its own specified mean
244 infectiousness and dispersion parameter k , and measure the
245 resulting basic reproductive numbers. In each case we let the
246 pathogen spread in an Erdős-Renyi network with a mean con-
247 nectivity of either 10 or 50, to simulate scenarios with either
248 a restricted or fairly open society. The results are shown in
249 Fig. 3, where the competitive (dis)advantage of each variant
250 is plotted as a function of its a given biological mean infec-
251 tiousness and dispersion. The infectiousness is given relative
252 to the SARS-CoV-2 ancestral strain which is set to average
253 infectiousness = 1 and has dispersion $k = 0.1$. This average
254 infectiousness of 1 corresponds to a basic reproduction number
255 of $R_0 = 3$ in a well-mixed scenario, representative of COVID-
256 19 (22). In the socially restricted case with only 10 contacts,
257 the competitive advantage depends strongly on the dispersion
258 parameter, as evidenced by the contour lines in Fig. 3A. The
259 dashed white contour in the figure indicates variants which
260 spread *as well* as the ancestral strain. Concretely, a variant
261 with just half the biological infectiousness of the ancestral
262 strain has no substantial competitive disadvantage, provided
263 it is sufficiently homogeneous ($k \gtrsim 1.0$). In the more socially
264 connected scenario (Fig. 3B), the competitiveness of a strain
265 is observed to depend less strongly on dispersion, and is pri-
266 marily determined by biological mean infectiousness. Viewed
267 more broadly, these results imply that an observed increase
268 in R_0 for an emerging variant may be due to a *combination*
269 of changes in transmission patterns (k) and biological mean
270 infectiousness

271 So far, our focus has been on mitigation strategies which
272 rely on reductions in contact network. However, even when
273 societies reopen by allowing contact with an increased num-
274 ber of individuals, non-pharmaceutical interventions which
275 decrease transmission risk per encounter may be in force.
276 These may include face masks and regular testing. In the
277 Supporting Information, we show that interventions which
278 decrease the transmission risk per encounter (i.e. per unit of

279 contact time) in fact decrease the competitive advantage of
280 more homogeneous variants. These types of interventions thus
281 have essentially the opposite effect, relative to strategies which
282 reduce social connectivity.

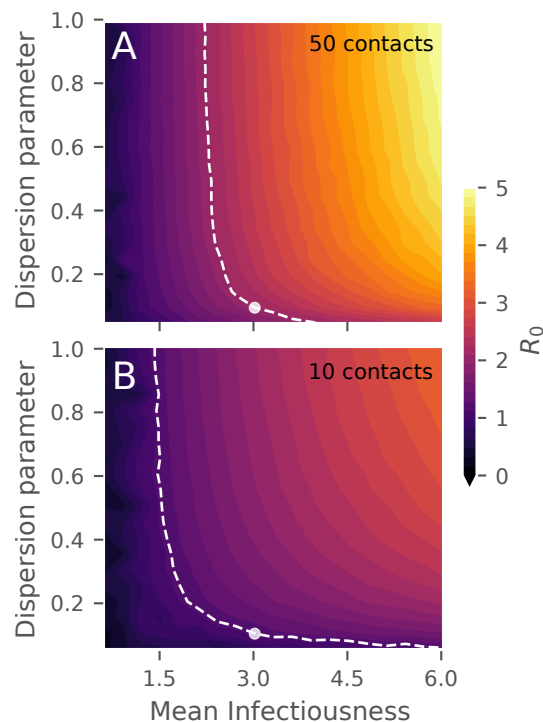


Fig. 3. Relative fitness of variants. The color indicates the basic reproductive number that each variant exhibits under the given circumstances. The dashed white line indicates variants which have the same fitness as the ancestral strain, which is estimated to have $k = 0.1$. The biological mean infectiousness (horizontal axis) has been scaled such that it equals the basic reproductive number (R_0) in a homogeneous mixing scenario. **A)** Spread of the disease in a connectivity 10 Erdős-Renyi network, corresponding to a partial lockdown. **B)** Spread of the disease in a connectivity 50 Erdős-Renyi network, corresponding to a mostly open society.

283 Interventions exert selection pressure

284 As the observed differences in the viral load distributions of
285 the Alpha (B.1.1.7.) variant and the ancestral strain suggest,
286 overdispersion is not a fixed property, but rather one that may
287 evolve over time. Furthermore, the SARS-CoV-2 pathogen
288 has been estimated to mutate at a rate of approximately 2
289 substitutions per genome per month (23), translating to about
290 one mutation per three transmissions. In Fig. 4, we explore
291 the consequences of overdispersion as an evolving feature of
292 the pathogen. In these simulations, the virus has a mutation
293 probability of 1/3 at each transmission. When it mutates, the
294 overdispersion factor is either increased (by a factor of 3/2) or
295 decreased (by a factor of 2/3). Thus, we assume no drift on
296 the microscopic scale, but one may arise macroscopically due
297 to selection pressure from the environment. It should of course
298 be noted that while the assumed mutation rate is realistic for
299 SARS-CoV-2, many mutations will be neutral and only very
300 few mutations will affect transmission dynamics. As such, the
301 present model will likely overestimate the *magnitude* of the
302 drift in overdispersion. It is however conceptually robust –
303 decreasing the mutation rate merely slows down the drift, but
304 the tendency remains.

305 In our simulations, we find that there is always a tendency

306 for overdispersion to decrease (i.e. for the k value to *increase*),
 307 leading to more homogeneous disease transmission. This makes
 308 sense, since we have already established that heterogeneous
 309 disease variants are more likely to undergo stochastic extinction
 310 (Fig. 1) and that they have a competitive disadvantage
 311 as soon as contact structures are anything but well-mixed
 312 (Fig. 3). In the absence of any interventions, the tendency
 313 to evolve towards homogeneity is quite weak (Fig. 4A), but
 314 when a partial lockdown is instituted, the picture changes
 315 dramatically and the k value increases exponentially. The
 316 conclusion is thus that lockdowns exert a selection pressure on
 317 the virus when it comes to overdispersion, towards developing
 318 a less superspreading-prone phenotype.
 319 One may of course object that the scenarios of Fig. 4A (un-
 320 restricted spread) and 4B (partial lockdown) are not directly
 321 comparable, since the epidemic in 4A unfolds much more
 322 rapidly. For this reason, we have included the scenario shown
 323 in 4C, where the transmission rate per encounter has been
 324 lowered, but social structure is unrestricted. The transmission
 325 rate is lowered such that the *initial* daily growth rates in Fig.
 326 4B and 4C are identical (11%/day averaged over the first 14
 327 days). This slightly increases the growth of k over the course of
 328 the epidemic, but to a much lower level than in the lockdown
 329 scenario, demonstrating that it is indeed the restriction of
 330 social network that provides the selection pressure driving k
 331 upwards.

332 Discussion

333 With this paper we have demonstrated that the relative success
 334 and survival of mutants of a superspreading disease depends on
 335 the type of mitigation strategies employed within a population.
 336 The choice of a certain mitigation strategy may well amount to
 337 selecting the next dominant variant. If, for example, a simple
 338 lockdown is enacted while still allowing people to meet within
 339 restricted social groups, the evolution of more homogeneously
 340 spreading disease variants may become favoured.

341 The spreading of an emerging virus in a human society is
 342 a complex phenomenon, where the actual reproductive number
 343 depends on sociocultural factors, mitigation policies and
 344 self-imposed changes in the behaviour of citizens as awareness
 345 grows in the population. The spread of a disease such as
 346 COVID-19 cannot simply be characterized by a single fitness
 347 quantity like the basic reproductive number R_0 , but will also
 348 depend on the heterogeneities of transmission patterns within
 349 the population. If schools are open, mutants which spread
 350 more easily among children may be selected for, whereas rapid
 351 self-isolation of infected individuals may tend to favor vari-
 352 ants which temporally separate disease transmission from the
 353 development of symptoms. We have focused on modeling the
 354 evolutionary effects of biological superspreading in the context
 355 of mitigations such as lockdowns which have been implemented
 356 globally during the COVID-19 pandemic. We found that such
 357 lockdowns will favour the emergence of homogeneously spread-
 358 ing variants over time.

359 Our findings also have implications for the assessment of
 360 new variants. They highlight the importance of taking overdis-
 361 persion into account when evaluating the transmissibility of an
 362 emerging variant. We have shown that the disease can spread
 363 more effectively not only by increasing its biological mean
 364 infectiousness, but also by changing its pattern of transmission
 365 to become more homogeneous. Practically, this means that

transmission data obtained under even partial lockdown can
 lead to an overestimation of the transmissibility of an emerging
 variant. We thus call for an increased focus on measuring the
 overdispersion of variants, as this may be critical for estimat-
 ing the reproductive number of new variants. These estimates
 in turn determine the required vaccination levels to reach herd
 immunity.

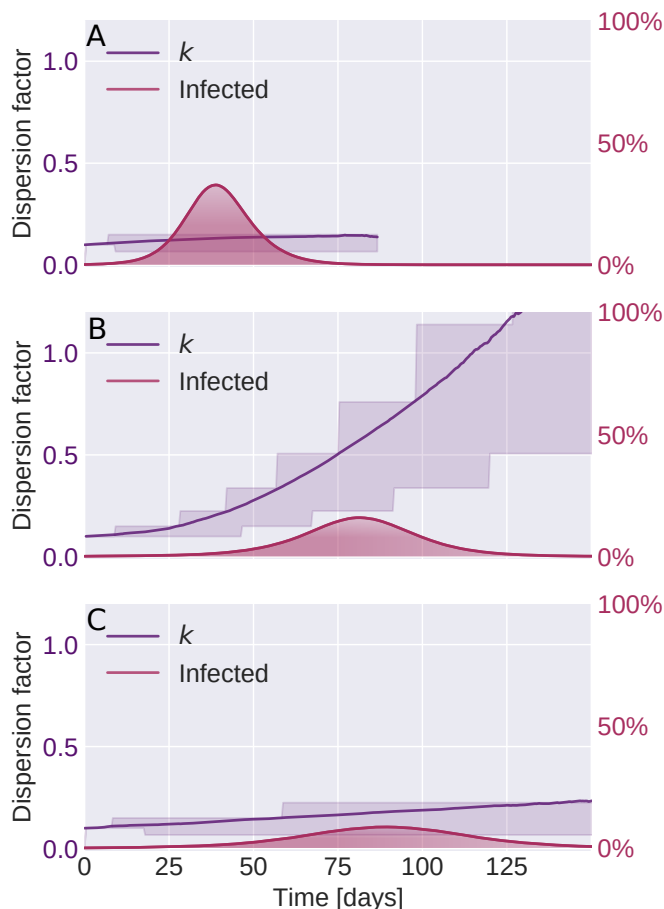


Fig. 4. Evolution of overdispersion is driven by imposed restrictions. In these simulations, random mutations occur which alter the level of transmission overdispersion in a non-directed fashion. However, external evolutionary pressures are seen to drive the disease towards developing more homogeneous spreading patterns. The filled red curve shows the combined incidence of all strains. The purple curve shows the average dispersion factor k in the infected population (with higher k corresponding to a more homogeneous infectiousness). The shaded purple area shows the 25% and 75% percentiles of the distribution of dispersion factors in the infected population. **A)** The pathogen evolves in an open society with no restrictions imposed (homogeneous mixing contact structure). **B)** Partial lockdown, with an average social network connectivity restricted to 15 persons. **C)** No restrictions on social network, but infectiousness lowered by other means (e.g. face masks).

Materials and Methods

We use an individual-based (or agent-based) network model of disease transmission as originally developed in Ref. (18). In this section, we present only a brief overview of the basic model, and refer to Ref. (18) for a more detailed description. We then go on to describe in detail the simulations and calculations which are particular to this manuscript.

The disease progression model consists of four overall states, **S**usceptible, **E**xposed, **I**nfected and **R**ecovered. The exposed state has an average duration of 2.4 days and is subdivided into two consecutive states with exponentially distributed waiting times (i.e.

384 having constant probability rate for leaving the state) of 1.2 days
 385 each, thus constituting a gamma distributed state when viewed as
 386 a whole. The infectious state is divided into two states as well, of
 387 1.2 and 5 days in duration, respectively.

388 Each individual in the model is associated with a fixed social
 389 network. Only a subset of edges are activated in each timestep, to
 390 simulate a contact event. In the simulations of this work, we always
 391 use either an Erdős-Renyi network with finite mean connectivity, or
 392 a homogeneous-mixing contact structure, which is also obtainable
 393 as the infinite connectivity limit of an Erdős-Renyi network.

394 When an edge connecting a susceptible and an infectious in-
 395 dividual is active, there is a certain probability per unit of time
 396 for disease transmission to occur. This rate is determined by the
 397 individual infectiousness r_i of the infectious agent, which is drawn
 398 from a gamma distribution with dispersion parameter k before the
 399 individual has become infectious. As such, the infectiousness for
 400 any given individual is assumed constant throughout the infectious
 401 stage of the disease. The infectiousness distribution determines an
 402 upper bound on size Δt of the timesteps in the model, since
 403 the inequality $r_i \cdot \Delta t < 1$ must hold for all agents. A timestep of
 404 size $\Delta t = 30\text{min}$ was used throughout, since this was sufficient to
 405 ensure that the inequality was satisfied.

406 Below we go into more detail as to how the simulations involving
 407 multiple strains were performed.

408 **Stochastic extinction.** The stochastic extinction (or, conversely, sur-
 409 vival) plots of Figure 1 in the main text rely entirely on a branching
 410 process algorithm with sampling of probability distributions with
 411 an analytic description. In practice, we have performed the compu-
 412 tation by numerical sampling.

413 In each generation of the epidemic, the computation is reiter-
 414 ated. Without loss of generality, we therefore here describe a single
 415 generation which initially has I infected individuals. Note that for
 416 the initial generation, $I = 1$ infected individuals.

- 417 • For $i \in \{1, \dots, I\}$:
 - 418 – Draw individual infectiousness ξ_i from Gamma distribu-
 419 tion $P_\xi(\xi; k, \mu)$
 - 420 – Draw number of contacts c from a Poisson distribution
 421 with a given mean connectivity.
 - 422 – Given number of contacts c , draw personal reproductive
 423 number z_i from the distribution Eq. (3)

$$424 P_z(z; \xi, c) = \binom{c}{z} (1 - e^{-\xi/c})^z (e^{-\xi/c})^{(c-z)}. \quad [3]$$

- 425 • Let the number of newly infected be $I = \sum_i z_i$ and repeat the
 426 algorithm with this new value of I .

427 If the number of infected I ever drops to zero, the outbreak is said
 428 to have undergone stochastic extinction in that generation. By
 429 performing multiple such branching process simulations for each
 430 value of the parameters μ (mean infectiousness) and k (dispersion
 431 factor) we build up a statistic of the survival chance of each specific
 432 variant. To generate Figure 1, this is repeated for two different
 433 values of the mean connectivity c .

434 **Two-strain competition simulations.** In Fig. 2, two strains spread
 435 simultaneously in the population of $N = 10^6$ individuals. Initially,
 436 0.99% of the population are infected with the heterogeneous "old"
 437 variant ($k = 0.1$), while 0.01% are infected with the more homo-
 438 geneous "new" variant ($k = 0.2$). Once a person with a given
 439 variant infects a susceptible individual, the characteristics of the
 440 variant are passed on to the newly infected individual, such that
 441 the infectiousness of this person is drawn from a Gamma distribu-
 442 tion with dispersion parameter k set by the variant. In other
 443 words, these simulations assume that no further mutations affecting
 444 overdispersion occur, allowing us to track solely the competition of
 445 two differently-dispersed variants within a population.

446 **Evolutionary model.** In Fig. 4, we allow the pathogen to stochasti-
 447 cally mutate upon transmission, with the mutations affecting the
 448 degree of overdispersion. In the simulations, the pathogen mutates
 449 on average once for each new host it is transmitted to (i.e. with

450 mutation probability $p = 1/3$) and the mutations are assumed to
 451 always affect overdispersion, by either increasing the k value by a
 452 factor of $3/2$ (i.e. $k \rightarrow 3k/2$) or decreasing it by a factor of $2/3$
 453 (i.e. $k \rightarrow 2k/3$). On a microscopic level, the dispersion level thus
 454 performs an unbiased (multiplicative) random walk. The value of
 455 this step-size parameter is arbitrarily chosen, and as such the simula-
 456 tions can only be regarded as qualitative and conceptual. However,
 457 although no intrinsic bias is built into the mutation mechanism,
 458 external selection pressures may drive the level of overdispersion in
 459 the population up or down, as is explored in Fig. 4.

460 In Fig. 4C, the average infectiousness of the strain is lowered so
 461 as to produce an initial growth rate that is identical to that of 4A,
 462 namely 11% per day in the first 14 days of the epidemic.

463 **ACKNOWLEDGMENTS.** We thank Robert J. Taylor, and Julius
 464 B. Kirkegaard for enlightening discussions. Our research has re-
 465 ceived funding from the European Research Council (ERC) under
 466 the European Union's Horizon 2020 research and innovation pro-
 467 gramme, grant agreement No. 740704, as well as from the Carlsberg
 468 Foundation under its Semper Ardens programme (grant # CF20-
 469 0046).

- 470 1. D Miller, et al., Full genome viral sequences inform patterns of SARS-CoV-2 spread into and
 471 within Israel. *Nat. communications* **11**, 1–10 (2020).
- 472 2. A Endo, S Abbott, AJ Kucharski, S Funk, , et al., Estimating the overdispersion in covid-19
 473 transmission using outbreak sizes outside china. *Wellcome Open Res.* **5**, 67 (2020).
- 474 3. C Pozderac, B Skinner, Superspreading of sars-cov-2 in the usa. *PLoS one* **16**, e0248808
 475 (2021).
- 476 4. JB Kirkegaard, K Sneppen, Variability of individual infectiousness derived from aggregate
 477 statistics of covid-19. *medRxiv* **0** (2021).
- 478 5. Q Yang, et al., Just 2% of sars-cov-2-positive individuals carry 90% of the virus circulating in
 479 communities. *Proc. Natl. Acad. Sci.* **118** (2021).
- 480 6. JO Lloyd-Smith, SJ Schreiber, PE Kopp, WM Getz, Superspreading and the effect of individ-
 481 ual variation on disease emergence. *Nature* **438**, 355–359 (2005).
- 482 7. AP Galvani, RM May, Dimensions of superspreading. *Nature* **438**, 293–295 (2005).
- 483 8. ME Woolhouse, et al., Heterogeneities in the transmission of infectious agents: implications
 484 for the design of control programs. *Proc. Natl. Acad. Sci.* **94**, 338–342 (1997).
- 485 9. C Fraser, DA Cummings, D Klinkenberg, DS Burke, NM Ferguson, Influenza transmission in
 486 households during the 1918 pandemic. *Am. journal epidemiology* **174**, 505–514 (2011).
- 487 10. J Brugger, CL Althaus, Transmission of and susceptibility to seasonal influenza in switzerland
 488 from 2003 to 2015. *Epidemics* **30**, 100373 (2020).
- 489 11. MG Roberts, H Nishiura, Early estimation of the reproduction number in the presence of
 490 imported cases: pandemic influenza h1n1-2009 in new zealand. *PLoS one* **6**, e17835 (2011).
- 491 12. MS Graham, et al., Changes in symptomatology, reinfection, and transmissibility associated
 492 with the sars-cov-2 variant b. 1.1. 7: an ecological study. *The Lancet Public Heal.* **6**, e335–
 493 e345 (2021).
- 494 13. E Volz, et al., Assessing transmissibility of sars-cov-2 lineage b. 1.1. 7 in england. *Nature*
 495 **593**, 266–269 (2021).
- 496 14. NG Davies, et al., Estimated transmissibility and impact of sars-cov-2 lineage b. 1.1. 7 in
 497 england. *Science* **372** (2021).
- 498 15. M Kidd, et al., S-variant SARS-CoV-2 lineage B.1.1.7 is associated with significantly higher
 499 viral loads in samples tested by ThermoFisher TaqPath RT-qPCR. *The J. infectious diseases*
 500 **223** (2021).
- 501 16. T Golubchik, et al., Early analysis of a potential link between viral load and the N501Y mu-
 502 tation in the SARS-COV-2 spike protein. *medRxiv* **0** (2021).
- 503 17. K Sneppen, BF Nielsen, RJ Taylor, L Simonsen, Overdispersion in COVID-19 increases the
 504 effectiveness of limiting nonrepetitive contacts for transmission control. *Proc. Natl. Acad. Sci.*
 505 **118** (2021).
- 506 18. BF Nielsen, L Simonsen, K Sneppen, COVID-19 superspreading suggests mitigation by so-
 507 cial network modulation. *Phys. Rev. Lett.* **126**, 118301 (2021).
- 508 19. A Kucharski, CL Althaus, The role of superspreading in middle east respiratory syndrome
 509 coronavirus (mers-cov) transmission. *Eurosurveillance* **20**, 21167 (2015).
- 510 20. BM Althouse, et al., Superspreading events in the transmission dynamics of sars-cov-2: Op-
 511 portunities for interventions and control. *PLoS biology* **18**, e3000897 (2020).
- 512 21. PZ Chen, et al., Heterogeneity in transmissibility and shedding sars-cov-2 via droplets and
 513 aerosols. *Elife* **10**, e65774 (2021).
- 514 22. A Billah, M Miah, N Khan, Reproductive number of coronavirus: A systematic review and
 515 meta-analysis based on global level evidence. *PLOS ONE* **15**, 1–17 (2020).
- 516 23. M Worobey, et al., The emergence of sars-cov-2 in europe and north america. *Science* **370**,
 517 564–570 (2020).